

Control of Spin State in (Porphinato)iron(III) Complexes. A New Crystalline Phase of (Isothiocyanato)(pyridine)(*meso*-tetraphenylporphinato)iron(III) with Two Magnetically Distinct Sites

David K. Geiger,¹ Vinai Chunplang,² and W. Robert Scheidt*¹

Received May 2, 1985

The preparation of a new phase of (isothiocyanato)(pyridine)(*meso*-tetraphenylporphinato)iron(III) is described. This triclinic phase differs from that previously described,⁶ in having substantially higher magnetic moments for the iron(III) center. The determination of the molecular structure by X-ray diffraction at 96 and 293 K and the temperature-dependent (~18–296 K) magnetic moments suggest that the best explanation of the structure and magnetism is given by a two-site model. One site of the [Fe(TPP)(NCS)(py)] molecule is a high-spin site under all conditions; the second site undergoes a low-spin–high-spin thermal equilibrium. The crystal structure determinations suggest possible reasons for the site discrimination. The magnetic moment at 296 K is 5.1 μ_B , decreasing to a minimum of about 4.4–4.5 μ_B . Crystal data for FeSN₆C₅₀H₃₃: triclinic, space group $P\bar{1}$, $Z = 2$; $a = 11.244$ (3) Å, $b = 17.132$ (4) Å, $c = 11.167$ (3) Å, $\alpha = 100.01$ (2)°, $\beta = 108.84$ (2)°, and $\gamma = 72.49$ (1)° at 96 K; $a = 11.423$ (2) Å, $b = 17.297$ (6) Å, $c = 11.324$ (2) Å, $\alpha = 99.98$ (2)°, $\beta = 109.43$ (1)°, and $\gamma = 72.43$ (2)° at 296 K.

Structural³ and magnetic⁴ characterization of (thiocyanato)-methemoglobin ((NCS)metHb) has been reported. The hemes exist in a thermal spin equilibrium ($S = 1/2$, $S = 5/2$); both human and horse derivatives are about 60% high-spin at room temperature.^{4a} Although the distribution of the high-spin fraction between the α and β subunits is not known with certainty, the distribution most consistent with crystallographic results is about 20% on the α -heme and 100% on the β -heme.³

We have recently reported the structural and physical characterization of the mixed-ligand complexes [Fe(OEP)(NCS)(py)] and [Fe(TPP)(NCS)(py)].^{5,6} The octaethylporphyrin complex is high-spin ($S = 5/2$, $\mu = 5.9 \mu_B$), while the tetraphenylporphyrin complex has a structure consistent with a low-spin ($S = 1/2$) state.⁷ However, the magnetic moment of the tetraphenylporphyrin complex is somewhat higher than expected for a low-spin complex and also shows temperature dependence. This suggests that [Fe(TPP)(NCS)(py)] is near the spin-crossover region. In iron(III) porphyrinates near the spin-crossover region, we have observed that a number of factors can influence the spin state of the porphinato derivative. These include an effect of the porphinato ligand,⁸ with more basic porphyrins favoring high-spin and less basic porphyrins favoring low-spin species. Thus, for [Fe(Porph)(3-Cl-py)₂]ClO₄, an increase in porphyrin basicity results in a larger fraction of high-spin molecules. Another important factor is an axial ligand orientation effect. [Fe(OEP)-(3-Cl-py)₂]ClO₄ displays three distinct spin states depending on temperature and crystalline state.^{9,10} A triclinic modification⁹ exists in thermal $S = 1/2$, $S = 5/2$ spin equilibrium and a monoclinic form¹⁰ exhibits an $S = 3/2$, $5/2$ quantum admixed intermediate-spin state. The differences in electronic state exhibited by the two crystalline modifications results from differences in the axial ligand orientation, which are enforced by crystal packing interactions.¹⁰ Finally, IEH MO calculations suggest that

Table I. Summary of Crystal Data and Intensity Collection Parameters for [Fe(TPP)(NCS)(py)]

<i>T</i> , K	293	96
formula	FeSN ₆ C ₅₀ H ₃₃	FeSN ₆ C ₅₀ H ₃₃
fw	805.8	805.8
cryst dimens, mm	0.65 × 0.37 × 0.17	0.62 × 0.80 × 0.40
space group	$P\bar{1}$	$P\bar{1}$
<i>a</i> , Å	11.423 (2)	11.244 (3)
<i>b</i> , Å	17.297 (6)	17.132 (4)
<i>c</i> , Å	11.324 (2)	11.167 (3)
α , deg	99.98 (2)	100.01 (2)
β , deg	109.43 (1)	108.84 (2)
γ , deg	72.43 (2)	72.49 (1)
<i>V</i> , Å ³	2005	1935
<i>Z</i>	2	2
<i>d</i> (calcd), g/cm ³	1.335	1.383
<i>d</i> (obsd), g/cm ³	1.336	
radiation ^a	Mo K α	Mo K α
scan technique	θ - 2θ	θ - 2θ
scan range	0.65 below K α_1 to 0.65 above K α_2	0.75 below K α_1 to 0.75 above K α_2
scan rate, deg/min	2–12	2–24
bkgd	0.5 times scan time at extreme of scan	profile analysis
2θ limits, deg	3.5–45.8	3.5–56.8
criterion for observn	$F_o > 3\sigma(F_o)$	$F_o > 3\sigma(F_o)$
no. of unique obsd data	4655	8938
μ , min ⁻¹	0.467	0.483
<i>R</i> ₁	0.118	0.130
<i>R</i> ₂	0.155	0.194
goodness of fit	4.22	6.22
data/parameter	9.8	18.5

^a Graphite monochromated; $\lambda = 0.71073$ Å.

for ferric porphyrinates that are not unambiguously low-spin species, high-, low-, and intermediate-spin states can be equienergetic.¹¹

We report herein the characterization of a second crystalline form of [Fe(TPP)(NCS)(py)]. This crystalline form differs from the previously reported hemipyridine solvate⁶ in having no solvate molecule and in having much higher magnetic moments, which also show some temperature dependence. The complex has been characterized by magnetochemical studies and multiple-temperature X-ray structure determinations. The data can be best explained in terms of two crystallographically and magnetically distinct lattice sites for [Fe(TPP)(NCS)(py)]. One site remains high-spin at all temperatures between ~96 and 293 K, the second site is a spin-equilibrium site under these conditions. These results

- (1) University of Notre Dame.
- (2) Rice University.
- (3) Korszun, Z. R.; Moffat, K. *J. Mol. Biol.* **1981**, *145*, 815–824.
- (4) (a) Perutz, M. R.; Sanders, J. K. M.; Chenery, D. H.; Noble, R. W.; Penelly, R. R.; Fung, L. W.-M.; Ho, C.; Giannini, I.; Porschke, D.; Winkler, H. *Biochemistry* **1978**, *17*, 3640–3652. (b) Messana, C.; Cerdonio, M.; Shenken, R.; Noble, R. W.; Fermi, G.; Perutz, R. N.; Perutz, M. F. *Biochemistry* **1978**, *17*, 3652–3662. (c) George, P.; Bettelstone, J.; Griffith, J. S. *Rev. Mod. Phys.* **1964**, *36*, 441–458.
- (5) Abbreviations used in this paper: TPP, dianion of *meso*-tetraphenylporphyrin; OEP, dianion of octaethylporphyrin; Porph, dianion of a generalized porphyrin; py, pyridine; 3-Cl-py, 3-chloropyridine; N_p, porphinato nitrogen atom; metHb, methemoglobin.
- (6) Scheidt, W. R.; Lee, Y. J.; Geiger, D. K.; Taylor, K.; Hatano, K. *J. Am. Chem. Soc.* **1982**, *104*, 3367–3374.
- (7) Scheidt, W. R.; Reed, C. A. *Chem. Rev.* **1981**, *81*, 543–555.
- (8) Geiger, D. K.; Scheidt, W. R. *Inorg. Chem.* **1984**, *23*, 1970–1972.
- (9) Scheidt, W. R.; Geiger, D. K.; Haller, K. J. *J. Am. Chem. Soc.* **1982**, *104*, 495–499.
- (10) Scheidt, W. R.; Geiger, D. K.; Hayes, R. G.; Lang, G. *J. Am. Chem. Soc.* **1983**, *105*, 2625–2632.

- (11) Scheidt, W. R.; Gouterman, M. In "Physical Bioinorganic Chemistry—Iron Porphyrins, Part I"; Lever, A. B. P., Gray, H. B., Eds.; Addison-Wesley: Reading, MA, 1983; pp 89–139.

further illustrate the sensitivity of spin state to the heme environment and the subtleties involved in spin-state determination.

Experimental Section

Synthesis and Magnetic Measurements of [Fe(TPP)(NCS)(py)]. All physical measurements were obtained on single-crystal specimens.¹² These were obtained in a manner analogous to that previously reported for the hemipyridine solvate:⁶ 100 mg of Fe(TPP)(NCS)¹³ was put into 2 mL of chloroform and 5 mL of pyridine (dried over 4-Å molecular sieves). Hexane vapor was allowed to slowly diffuse into the chloroform solution. Single crystals formed on the sides of the crystallization vessel. Single crystals of the hemipyridine solvate were obtained by changing the nonsolvent from pure hexane to 30% (v/v) diethylether in pentane. Magnetic susceptibilities were measured on a Faraday balance described previously¹⁴ with the following modifications for improved temperature control. The balance was equipped with a Scientific Instruments Model 3800 Temperature indicator/controller and a LFE Model 4247 voltmeter monitoring a Scientific Instruments Si-400 silicon diode sensor.

Structure Determinations. Preliminary X-ray study of crystals of [Fe(TPP)(NCS)(py)] on a Nicolet PI automated diffractometer established a two-molecule triclinic unit cell. A Delaunay reduction did not show any hidden symmetry. Crystal data and intensity collection parameters from the complex at 293 and 96 K are given in Table I. Low-temperature diffraction data were measured by using a LT-1 attachment to the diffractometer. The intensities of four standard reflections were measured every 50 reflections to monitor the alignment and possible deterioration of the crystal during data collection. No significant variation in the standard reflections was observed. Intensity data were reduced as previously described.¹⁵

Initial structure solution was attempted in the centrosymmetric space group $P\bar{1}$, and the structure was solved by using the direct methods program MULTAN78.¹⁶ Rather than the expected single molecule in a general position, two half-molecules were found around the inversion centers at 0, 0, 0 and 0, $\frac{1}{2}$, $\frac{1}{2}$. Patterson calculations with both the room-temperature and the low-temperature data sets also showed two iron atoms separated by the vector 0, $\frac{1}{2}$, $\frac{1}{2}$. The choice of $P\bar{1}$ as the space group appears to be the proper choice (vide infra). Thus, there are two independent half-molecules, each with crystallographically required inversion centers, in the asymmetric unit. Consequently, the axial ligands must be disordered as a result of the crystallographically required symmetry. We were thus presented with a difficult refinement problem. Indeed, although all the atoms of the axial ligands were found in difference Fourier maps, attempts at unconstrained refinement were unsuccessful owing to high correlation between axial ligand atoms. Therefore, the model employed for least-squares refinement used rigid-group descriptions for the pyridine and isothiocyanate ligands, each with an occupancy of 0.5. The rigid-group descriptions of the pyridine and isothiocyanate ligands were obtained from the structures of the hemipyridine solvate and the OEP analogue.⁶ Individual isotropic thermal parameters for the thiocyanate atoms were refined, but single-group isotropic thermal parameters were used for the pyridine ligands. The thermal parameters for each iron atom were large ($B = 4.3$ and 5.0 \AA^2), suggesting positional disorder of iron about the inversion centers. They were thus placed 0.2 Å out of the respective porphyrin planes and allowed to refine unconstrained. Placing the iron atoms out of the plane resulted in a problem that was never quite resolved: the irons moved slightly off center so that the line joining an iron atom with its inversion center related atom was not perpendicular to the porphyrin plane. Attempts to refine both the coordinates and anisotropic temperature factors for the iron atoms led to nonpositive-definite temperature factors. Accordingly, the iron atoms were refined with isotropic temperature factors. Anisotropic refinement was carried out for all other heavy atoms not associated with the rigid groups. All hydrogen atoms were located by using difference Fourier maps and were included in subsequent cycles of least-squares refinement as fixed contributors. Final atomic positional parameters for the room-temperature structure are listed in Table II.

Table II. Fractional Coordinates for [Fe(TPP)(NCS)(py)] at 293 K^a

atom	x	y	z
Fe(1)	-0.0082 (4)	0.0104 (2)	0.0023 (4)
Fe(2)	-0.0213 (2)	0.5094 (2)	0.5021 (3)
N(1)	-0.1855 (6)	0.0055 (4)	-0.1006 (6)
N(2)	-0.0154 (6)	0.1061 (4)	-0.0628 (6)
C(m1)	-0.2378 (8)	0.1323 (6)	-0.2023 (7)
C(m2)	0.2047 (8)	0.1214 (5)	0.0453 (7)
C(a1)	-0.2516 (8)	-0.0496 (5)	-0.1068 (7)
C(a2)	-0.2667 (8)	0.0630 (5)	-0.1787 (7)
C(a3)	-0.1199 (7)	0.1514 (5)	-0.1468 (7)
C(a4)	0.0792 (8)	0.1465 (5)	-0.0341 (7)
C(b1)	-0.3783 (8)	-0.0245 (6)	-0.1874 (8)
C(b2)	-0.3862 (8)	0.0435 (6)	-0.2315 (8)
C(b3)	-0.0943 (8)	0.2218 (5)	-0.1701 (7)
C(b4)	0.0274 (8)	0.2195 (5)	-0.1014 (8)
C(11)	-0.3394 (7)	0.1851 (5)	-0.3004 (8)
C(12)	-0.3415 (11)	0.1665 (7)	-0.4238 (9)
C(13)	-0.4404 (13)	0.2133 (8)	-0.5167 (10)
C(14)	-0.5296 (10)	0.2758 (8)	-0.4889 (11)
C(15)	-0.5261 (9)	0.2986 (7)	-0.3609 (11)
C(16)	-0.4302 (10)	0.2514 (7)	-0.2690 (9)
C(21)	0.2958 (8)	0.1718 (5)	0.0610 (7)
C(22)	0.3917 (9)	0.1454 (6)	0.0029 (9)
C(23)	0.4721 (10)	0.1964 (9)	0.0193 (13)
C(24)	0.4617 (12)	0.2699 (9)	0.0944 (12)
C(25)	0.3690 (11)	0.2928 (6)	0.1461 (9)
C(26)	0.2858 (9)	0.2462 (6)	0.1307 (8)
N(3)	0.0171 (6)	0.3975 (4)	0.3765 (6)
N(4)	0.1001 (6)	0.4287 (4)	0.6460 (6)
C(m3)	0.1287 (8)	0.2927 (5)	0.5320 (8)
C(m4)	0.1144 (8)	0.5391 (6)	0.8181 (7)
C(a5)	-0.0459 (8)	0.3945 (5)	0.2491 (7)
C(a6)	0.0665 (8)	0.3179 (5)	0.4082 (7)
C(a7)	0.1478 (8)	0.3448 (5)	0.6413 (8)
C(a8)	0.1402 (8)	0.4589 (6)	0.7702 (7)
C(b5)	-0.0302 (8)	0.3123 (5)	0.1978 (7)
C(b6)	0.0357 (9)	0.2647 (5)	0.2942 (7)
C(b7)	0.2200 (9)	0.3204 (6)	0.7639 (8)
C(b8)	0.2174 (9)	0.3862 (6)	0.8426 (8)
C(31)	0.1771 (9)	0.2028 (5)	0.5496 (8)
C(32)	0.2618 (9)	0.1498 (6)	0.4922 (8)
C(33)	0.3119 (9)	0.0680 (7)	0.5170 (10)
C(34)	0.2643 (12)	0.0426 (6)	0.6029 (11)
C(35)	0.1824 (12)	0.0944 (7)	0.6555 (9)
C(36)	0.1330 (10)	0.1720 (6)	0.6291 (9)
C(41)	0.1791 (9)	0.5514 (5)	0.9571 (8)
C(42)	0.1039 (11)	0.5654 (6)	1.0386 (9)
C(43)	0.1613 (17)	0.5694 (7)	1.1691 (11)
C(44)	0.2879 (20)	0.5655 (8)	1.2115 (12)
C(45)	0.3632 (13)	0.5535 (10)	1.1350 (16)
C(46)	0.3009 (13)	0.5497 (8)	1.0044 (11)

^aThe estimated standard deviations of the least significant digits are given in parentheses.

Table A, final anisotropic temperature factors, Table B, fixed hydrogen atom positions, Table C, derived coordinates of the axial ligand rigid groups, and observed and calculated structure amplitudes ($\times 10$) are available as supplementary material.

The structure was also determined at 96 K. The previously determined coordinates of the 293 K structure were used to establish phases. The out-of-plane displacement of Fe(1) decreased to less than 0.06 Å, and so it was placed on the inversion center at 0, 0, 0. Fe(1) was successfully refined anisotropically, but attempts to refine the other iron atom using anisotropic temperature factors failed. The rigid-group constraints of the pyridine ligands were relaxed slightly: the atoms were refined with independent isotropic thermal parameters. Attempts to refine the structure in the noncentric space group $P\bar{1}$ (two complete molecules in the asymmetric unit) were attempted, but the pseudosymmetry associated with the 0, 0, 0 and 0, $\frac{1}{2}$, $\frac{1}{2}$ positions prevented any meaningful refinement of ordered axial ligands (vide infra). The final atomic coordinates are given in Table III. Table D, final values of the anisotropic thermal parameters, Table E, fixed hydrogen atom positions, and Table F, derived coordinates of the axial ligand rigid groups, and listings of observed and calculated structure factor amplitudes ($\times 10$) are available as supplementary material.

Considerable effort was expended in trying to assure that the correct choice of space group had been made, namely that $P\bar{1}$, with the attendant

- (12) Magnetic susceptibility measurements were performed on crushed single-crystal specimens (to ensure the presence of a single crystalline phase).
- (13) Maricondi, C.; Swift, W.; Straub, D. K. *J. Am. Chem. Soc.* **1969**, *91*, 5205-5210.
- (14) Tweedle, M. F.; Wilson, L. J.; Garcia-Inigues, L.; Babcock, G. T.; Plamer, G. *J. Biol. Chem.* **1978**, *253*, 8065-8073.
- (15) Scheidt, W. R. *J. Am. Chem. Soc.* **1974**, *96*, 84-89.
- (16) All intensity statistics were consistent with the centrosymmetric choice. Programs used in this study included local modifications of Main, Hull, Lessinger, Germain, Declercq, and Woolfson's MULTAN78, Jacobson's ALLF and ALLS, Busing and Levy's ORFFE and ORFLS, and Johnson's ORTEP2.

Table III. Fractional Coordinates for [Fe(TPP)(NCS)(py)] at 96 K^a

atom	x	y	z
Fe(1)	0.0	0.0	0.0
Fe(2)	-0.02047 (12)	0.51105 (8)	0.50233 (14)
N(1)	-0.1842 (4)	0.00524 (25)	-0.0997 (3)
N(2)	-0.0155 (4)	0.10549 (26)	-0.0614 (3)
C(m1)	-0.2426 (5)	0.1339 (3)	-0.2017 (4)
C(m2)	0.2064 (5)	0.1221 (3)	0.0447 (4)
C(a1)	-0.2532 (4)	-0.0504 (3)	-0.1049 (4)
C(a2)	-0.2690 (4)	0.0649 (3)	-0.1775 (4)
C(a3)	-0.1227 (4)	0.1525 (3)	-0.1443 (4)
C(a4)	0.0800 (5)	0.1474 (3)	-0.0322 (4)
C(b1)	-0.3843 (5)	-0.0230 (3)	-0.1873 (4)
C(b2)	-0.3951 (5)	0.0467 (4)	-0.2311 (5)
C(b3)	-0.0940 (5)	0.2228 (3)	-0.1690 (4)
C(b4)	0.0296 (5)	0.2211 (3)	-0.0982 (4)
C(11)	-0.3437 (5)	0.1866 (3)	-0.3002 (4)
C(12)	-0.3475 (6)	0.1660 (4)	-0.4271 (5)
C(13)	-0.4399 (8)	0.2117 (5)	-0.5200 (5)
C(14)	-0.5297 (7)	0.2757 (5)	-0.4907 (6)
C(15)	-0.5292 (6)	0.2999 (5)	-0.3638 (6)
C(16)	-0.4351 (6)	0.2515 (5)	-0.2709 (5)
C(21)	0.2987 (5)	0.1740 (3)	0.0611 (4)
C(22)	0.3991 (6)	0.1456 (4)	0.0049 (5)
C(23)	0.4826 (7)	0.1940 (5)	0.0177 (7)
C(24)	0.4690 (6)	0.2708 (4)	0.0929 (7)
C(25)	0.3719 (6)	0.2968 (3)	0.1477 (5)
C(26)	0.2846 (5)	0.2506 (3)	0.1342 (4)
N(3)	0.0177 (4)	0.3956 (3)	0.3759 (4)
N(4)	0.1002 (5)	0.4284 (3)	0.6460 (4)
C(m3)	0.1305 (6)	0.2910 (4)	0.5314 (5)
C(m4)	0.1171 (5)	0.5400 (4)	0.8224 (5)
C(a5)	-0.0451 (5)	0.3936 (4)	0.2488 (5)
C(a6)	0.0674 (5)	0.3159 (4)	0.4086 (5)
C(a7)	0.1497 (6)	0.3435 (4)	0.6417 (5)
C(a8)	0.1424 (5)	0.4575 (4)	0.7718 (4)
C(b5)	-0.0321 (6)	0.3084 (4)	0.1968 (5)
C(b6)	0.0375 (6)	0.2611 (4)	0.2954 (5)
C(b7)	0.2224 (6)	0.3209 (4)	0.7673 (5)
C(b8)	0.2176 (6)	0.3902 (4)	0.8468 (5)
C(31)	0.1778 (6)	0.2009 (4)	0.5507 (5)
C(32)	0.2632 (5)	0.1472 (4)	0.4905 (5)
C(33)	0.3103 (6)	0.0649 (4)	0.5164 (6)
C(34)	0.2702 (6)	0.0366 (4)	0.6051 (5)
C(35)	0.1867 (7)	0.0903 (4)	0.6638 (5)
C(36)	0.1378 (6)	0.1700 (4)	0.6354 (5)
C(41)	0.1770 (6)	0.5531 (4)	0.9630 (5)
C(42)	0.1002 (6)	0.5668 (4)	1.0458 (5)
C(43)	0.1580 (8)	0.5682 (4)	1.1754 (5)
C(44)	0.2851 (8)	0.5635 (5)	1.2251 (6)
C(45)	0.3582 (7)	0.5526 (6)	1.1454 (8)
C(46)	0.3062 (7)	0.5473 (5)	1.0099 (7)

^aThe estimated standard deviations of the least significant digits are given in parentheses.

axial ligand disorder, rather than *P1*, which in principle could be ordered, was the appropriate group. Both data sets were used in these tests; however, the low-temperature data set, with its concomitant lower thermal parameters and higher data/parameter ratio, was emphasized. Attempts to refine¹⁷ the structural parameters in space group *P1*, with all permutations of axial ligand and out-of-plane iron atom positions used as starting points, were judged unsuccessful owing to large correlations between parameters of pseudosymmetrically related atoms within each molecule. Various attempts¹⁸ to solve the structure in the noncentrosymmetric space group showed that all peripheral groups (both phenyl rings and axial ligands) retained a centrosymmetric arrangement within each molecule. We concluded that the proper choice of space group was made.

Results and Discussion

The fact that we had prepared a new crystalline phase of [Fe(TPP)(NCS)(py)] became known to us after a determination of the magnetic moment. The room-temperature magnetic moment was found to be near 5 μ_B , considerably higher than that

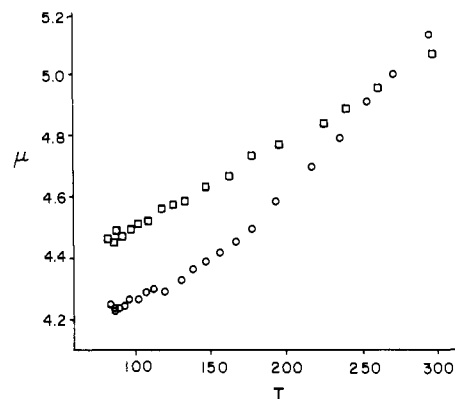


Figure 1. Magnetic moments vs. *T* for two separate preparations of triclinic [Fe(TPP)(NCS)(py)] from 84 to 293 K. The uncertainty in μ is $\pm 0.05 \mu_B$.

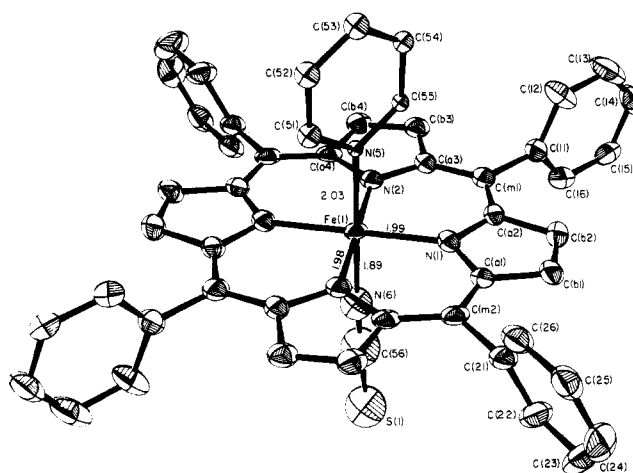


Figure 2. ORTEP plot of molecule 1 at 96 K. Atoms were plotted with 50% probability ellipsoids. The numbering system for the crystallographically unique atoms of the molecule is displayed.

observed for the hemipyridine crystalline phase.⁶ Which particular crystalline phase is prepared depends only on the nature of the nonsolvent used in the crystallization experiment. The reproducibility of the preparation of the two crystalline forms is consistently successful according to the nonsolvent combination used (cf. Experimental Section). Magnetic moments as a function of temperature were initially measured over the temperature range 84–293 K. The variation of the magnetic moments from 5.1 μ_B at room temperature to 4.4 μ_B at 84 K suggested that this crystalline form of the complex exhibited spin-crossover behavior typical of a number of iron(III) complexes. A second set of measurements on a new preparation of the complex, over the same temperature range, gave slightly different values for the magnetic moments, as shown in Figure 1. Such differences in magnetic moments between different samples and sample preparations have been commented on previously.¹⁹ Although this magnetic data would appear consistent with a simple spin equilibrium, the room-temperature crystal structure determination unexpectedly showed that there were two crystallographically distinct molecular sites. It should be noted that the two crystallographically distinct molecular sites are obtained from *either* space group choice. Despite some crystallographic difficulties, the results suggested that there were magnetic differences between the two sites. This led us to pursue the structure of the complex at a lower temperature as well. The low-temperature (96 K) structural results lead to the conclusion (vide infra) that there are two magnetically distinct sites in the lattice: one site remains high spin and the second is a spin-equilibrium site. We outline below the structural

(17) Full-matrix techniques were used in all cases.

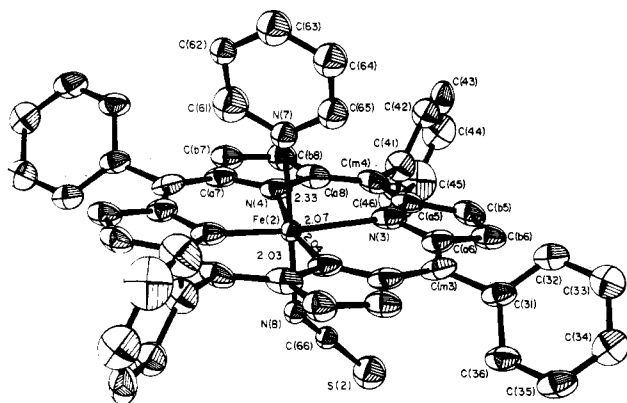
(18) These included de novo solutions using MULTAN and partial difference Fourier procedures.

(19) Haddad, M. S.; Federer, W. D.; Lynch, M. W.; Hendrickson, D. N. *Inorg. Chem.* **1981**, *20*, 131–139.

Table IV. Bond Distances in [Fe(TPP)(NCS)(py)]^a

type	dist, Å	type	dist, Å	type	dist, Å	type	dist, Å
Fe(1)-N(1) ^b	2.034 ^c	Fe(2)-N(3)	2.072 ^c	C(b1)-C(b2)	1.323 (11)	C(b5)-C(b6)	1.351 (11)
	1.993 (4)		2.073 ^c		1.326 (7)		1.361 (8)
Fe(1)-N(2)	2.023 ^c	Fe(2)-N(4)	2.052 ^c	C(b3)-C(b4)	1.340 (11)	C(b7)-C(b8)	1.317 (12)
	1.983 (4)		2.040 ^c		1.353 (7)		1.351 (8)
Fe(1)-N(5)	2.216	Fe(2)-N(7)	2.402	C(m1)-C(11)	1.507 (11)	C(m3)-C(31)	1.511 (12)
	2.027		2.328		1.496 (7)		1.502 (8)
Fe(1)-N(6)	1.908	Fe(2)-N(8)	1.970	C(m2)-C(21)	1.498 (11)	C(m4)-C(41)	1.508 (11)
	1.887		2.030		1.509 (6)		1.501 (7)
N(1)-C(a1)	1.364 (10)	N(3)-C(a5)	1.381 (10)	C(11)-C(12)	1.372 (12)	C(31)-C(32)	1.369 (12)
	1.382 (6)		1.366 (6)		1.390 (7)		1.375 (8)
N(1)-C(a2)	1.354 (10)	N(3)-C(a6)	1.383 (10)	C(12)-C(13)	1.411 (14)	C(32)-C(33)	1.398 (13)
	1.377 (6)		1.376 (7)		1.365 (9)		1.395 (9)
N(2)-C(a3)	1.372 (10)	N(4)-C(a7)	1.386 (10)	C(13)-C(14)	1.316 (14)	C(33)-C(34)	1.440 (16)
	1.383 (6)		1.392 (8)		1.324 (10)		1.416 (9)
N(2)-C(a4)	1.382 (10)	N(4)-C(a8)	1.387 (10)	C(14)-C(15)	1.426 (15)	C(34)-C(35)	1.310 (14)
	1.389 (6)		1.384 (6)		1.405 (9)		1.351 (9)
C(a1)-C(m2)	1.401 (11)	C(a5)-C(m4)	1.370 (11)	C(15)-C(16)	1.395 (13)	C(35)-C(36)	1.334 (13)
	1.381 (7)		1.389 (8)		1.395 (9)		1.362 (9)
C(a1)-C(b1)	1.413 (11)	C(a5)-C(b5)	1.421 (11)	C(16)-C(11)	1.379 (12)	C(36)-C(31)	1.406 (12)
	1.449 (7)		1.455 (8)		1.342 (8)		1.403 (7)
C(a2)-C(m1)	1.423 (11)	C(a6)-C(m3)	1.422 (11)	C(21)-C(22)	1.384 (12)	C(41)-C(42)	1.406 (13)
	1.390 (7)		1.400 (7)		1.388 (7)		1.405 (8)
C(a2)-C(b2)	1.414 (11)	C(a6)-C(b6)	1.455 (11)	C(22)-C(23)	1.405 (15)	C(42)-C(43)	1.402 (15)
	1.456 (6)		1.447 (7)		1.389 (8)		1.381 (8)
C(a3)-C(m1)	1.397 (11)	C(a7)-C(m3)	1.395 (10)	C(23)-C(24)	1.399 (16)	C(43)-C(44)	1.347 (20)
	1.400 (6)		1.390 (8)		1.426 (10)		1.377 (10)
C(a3)-C(b3)	1.419 (11)	C(a7)-C(b7)	1.420 (11)	C(24)-C(25)	1.304 (15)	C(44)-C(45)	1.364 (21)
	1.428 (7)		1.430 (7)		1.345 (9)		1.351 (12)
C(a4)-C(m2)	1.397 (11)	C(a8)-C(m4)	1.379 (11)	C(25)-C(26)	1.374 (13)	C(45)-C(46)	1.413 (18)
	1.384 (7)		1.408 (8)		1.395 (7)		1.433 (10)
C(a4)-C(b4)	1.453 (11)	C(a8)-C(b8)	1.496 (12)	C(26)-C(21)	1.381 (11)	C(46)-C(41)	1.307 (14)
	1.444 (7)		1.428 (8)		1.414 (7)		1.355 (10)

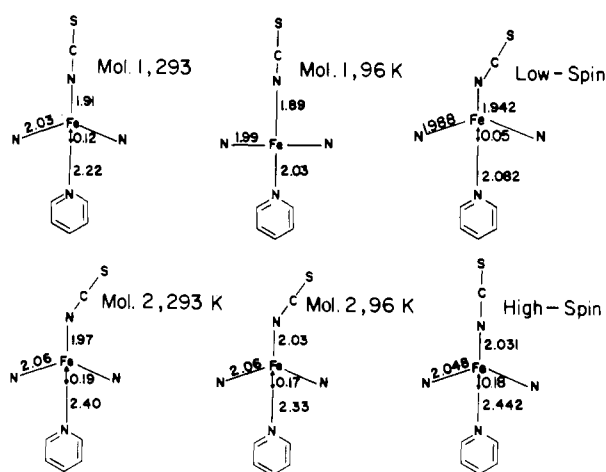
^aThe numbers in parentheses are estimated standard deviations. Distances without standard deviations are derived values. ^bFor each distance, the first line gives atomic distances at 293 K and the second line gives distances at 96 K. ^cThis value is the average distance using the two iron atoms related by the centers of symmetry.

**Figure 3.** ORTEP plot of molecule 2 at 96 K. The same information as in Figure 2 is given.

description of the two complexes and the evidence therefrom for this conclusion.

The structure of the two crystallographically independent molecules, determined at 293 K, are displayed in Figures 1S and 2S of the supplementary material. The two distinct molecules are designated as molecule 1 and molecule 2. Figures 2 and 3 display the structures of the two unique molecules, determined at 96 K, along with the labeling scheme and the bond distances in the coordination groups. Listings of individual bond distances and angles at 96 K and 293 K are given in Tables IV and V, respectively.

A comparison of the coordination groups of molecules 1 and 2, at 96 and 293 K, along with the structural parameters of the known high- and low-spin forms of [Fe(Porph)(NCS)(py)], is given in Figure 4. The average Fe-N_p distance of 2.06 Å found in molecule 2 at both temperatures is indicative of an occupied d_{x²-y²} orbital; the comparatively long axial bond distances are evidence of an occupied d_{z²} orbital.⁷ In fact, for molecule 2,

**Figure 4.** A comparison of structures of the [Fe(Porph)(NCS)(py)] molecules. Column 1 displays average parameters for the two molecules of this work at 293 K, column 2 that at 96 K, and column 3 the structure of low-spin [Fe(TPP)(NCS)(py)] and the structure of high-spin [Fe(OEP)(NCS)(py)], which are both described in ref 6.

$\langle \text{Fe-N} \rangle_{\text{av}}$ is 2.12 Å at both temperatures, which is in good agreement with the observed value of 2.11 Å in high-spin [Fe(OEP)(NCS)(py)].⁶ Thus, the crystallographic results provide good evidence that molecule 2 is in a high-spin state at both 96 and 293 K.

An examination of Figure 4 reveals that the coordination group geometry of molecule 1 is quite different from that of molecule 2 and that the molecule undergoes significant structural reorganization with a change in temperature. The average Fe-N_p bond distance of 1.99 Å obtained at 96 K is consistent with an unoccupied d_{x²-y²} orbital.⁷ The shorter axial bond lengths suggest that the d_{z²} orbital is also unoccupied at 96 K. In molecule 1, the average Fe-N_p bond length is 1.99 Å, the same as that found in

Table V. Bond Angles in $[\text{Fe}(\text{TPP})(\text{NCS})(\text{py})]^\circ$

type	angle, deg	type	angle, deg	type	angle, deg	type	angle, deg
N(1)Fe(1)N(2) ^b	95.0 (3) 90.1 (2)	N(3)Fe(2)N(4)	91.0 (3) 91.7 (2)	C(a3)C(m1)C(11)	118.3 (8) 119.2 (4)	C(a7)C(m3)C(31)	116.1 (7) 115.3 (5)
N(1)Fe(1)N(6)	92.6 90.9	N(3)Fe(2)N(8)	99.4 98.9	C(a2)C(m2)C(a4)	123.4 (7) 123.0 (4)	C(a5)C(m4)C(a8)	126.5 (7) 124.5 (5)
N(1)Fe(1)N(5)	89.1 89.4	N(3)Fe(2)N(7)	80.4 79.6	C(a1)C(m2)C(21)	118.1 (7) 118.3 (4)	C(a5)C(m4)C(41)	119.4 (8) 120.5 (5)
N(2)Fe(1)N(6)	89.4 89.3	N(4)Fe(2)N(8)	95.0 94.2	C(a4)C(m2)C(21)	118.4 (8) 118.7 (5)	C(a8)C(m4)C(41)	114.0 (8) 115.0 (5)
N(2)Fe(1)N(5)	89.8 89.9	N(4)Fe(2)N(7)	85.8 85.0	C(a1)C(b1)C(b2)	106.4 (8) 108.4 (4)	C(a5)C(b5)C(b6)	107.3 (7) 106.7 (5)
C(a1)N(1)C(a2)	106.5 (7) 105.9 (4)	C(a5)N(2)C(a6)	106.6 (6) 107.8 (5)	C(a2)C(b2)C(b1)	108.8 (7) 106.7 (4)	C(a6)C(b6)C(b5)	107.7 (8) 107.5 (5)
C(a3)N(2)C(a4)	105.4 (7) 105.1 (4)	C(a7)N(4)C(a8)	107.7 (7) 106.2 (5)	C(a3)C(b3)C(b4)	106.5 (7) 107.1 (5)	C(a7)C(b7)C(b8)	108.0 (8) 108.1 (5)
N(1)C(a1)C(b1)	109.7 (8) 109.1 (4)	N(3)C(a5)C(b5)	110.1 (7) 109.1 (5)	C(a4)C(b4)C(b3)	107.9 (7) 107.2 (4)	C(a8)C(b8)C(b7)	108.7 (8) 107.3 (5)
N(1)C(a1)C(m2)	126.9 (7) 126.6 (4)	N(3)C(a5)C(m4)	125.0 (7) 127.3 (5)	C(11)C(12)C(13)	119.1 (10) 121.1 (6)	C(31)C(32)C(33)	121.9 (9) 120.2 (5)
N(1)C(a2)C(b2)	108.6 (7) 109.9 (4)	N(3)C(a6)C(b6)	108.2 (7) 108.8 (5)	C(12)C(13)C(14)	122.3 (11) 120.3 (5)	C(32)C(33)C(34)	115.5 (9) 119.9 (6)
N(1)C(a2)C(m1)	125.9 (7) 126.6 (4)	N(3)C(a6)C(m3)	125.7 (7) 126.2 (5)	C(13)C(14)C(15)	119.6 (10) 121.0 (6)	C(33)C(34)C(35)	121.2 (10) 119.2 (6)
N(2)C(a3)C(b3)	111.5 (7) 110.8 (4)	N(4)C(a7)C(b7)	109.8 (7) 108.8 (5)	C(14)C(15)C(16)	118.3 (10) 117.5 (6)	C(34)C(35)C(36)	122.7 (10) 120.8 (5)
N(2)C(a3)C(m1)	125.0 (8) 126.0 (5)	N(4)C(a7)C(m3)	124.8 (7) 124.3 (5)	C(15)C(16)C(11)	121.1 (9) 121.6 (5)	C(35)C(36)C(31)	119.8 (9) 121.8 (6)
N(2)C(a4)C(b4)	108.7 (7) 109.8 (4)	N(4)C(a8)C(b8)	105.7 (8) 109.6 (5)	C(16)C(11)C(12)	119.5 (8) 118.4 (5)	C(36)C(31)C(32)	118.5 (8) 118.1 (5)
N(2)C(a4)C(m2)	126.1 (8) 126.1 (4)	N(4)C(a8)C(m4)	127.6 (8) 126.9 (5)	C(21)C(22)C(23)	117.4 (10) 119.6 (6)	C(41)C(42)C(43)	120.4 (12) 120.0 (6)
C(m1)C(a2)C(b2)	125.5 (8) 123.5 (5)	C(m3)C(a6)C(b6)	126.0 (8) 125.0 (5)	C(22)C(23)C(24)	122.9 (10) 120.3 (6)	C(42)C(43)C(44)	117.2 (13) 121.3 (6)
C(m1)C(a3)C(b3)	123.5 (8) 123.2 (5)	C(m3)C(a7)C(b7)	125.4 (8) 126.9 (6)	C(23)C(24)C(25)	117.5 (11) 119.2 (5)	C(43)C(44)C(45)	123.9 (13) 118.6 (6)
C(m2)C(a1)C(b1)	123.4 (8) 124.3 (4)	C(m4)C(a5)C(b5)	124.8 (8) 123.4 (5)	C(24)C(25)C(26)	121.9 (10) 121.9 (5)	C(44)C(45)C(46)	116.6 (13) 123.3 (7)
C(m2)C(a4)C(b4)	125.8 (8) 124.1 (4)	C(m4)C(a8)C(b8)	126.8 (8) 123.5 (5)	C(25)C(26)C(21)	122.3 (9) 119.1 (5)	C(45)C(46)C(41)	122.6 (13) 116.4 (4)
C(a2)C(m1)C(a3)	124.6 (8) 122.7 (5)	C(a6)C(m3)C(a7)	125.2 (8) 125.2 (6)	C(26)C(21)C(22)	117.9 (9) 119.9 (5)	C(46)C(41)C(42)	118.9 (10) 120.2 (6)
C(a2)C(m1)C(11)	117.0 (7) 118.0 (4)	C(a6)C(m3)C(31)	118.7 (8) 119.4 (5)				

^aThe numbers in parenthesis are the estimated standard deviations. Angles without standard deviations are derived values. ^bFor each angle, the first line gives angles from data collected at 293 K and the second line gives angles from data collected at 96 K.

the hemipyridine solvate, 1.988 Å, and strongly suggests that molecule 1 is low-spin ($S = 1/2$) at 96 K. At 293 K, molecule 1 has an average Fe–N_p bond distance of 2.03 Å, about midway between that expected for the high- and low-spin forms. The axial bond distances also fall between the values found for analogous high- and low-spin complexes. Finally, a significant out-of-plane displacement of the iron atom from the porphyrato core is observed at 293 K. The change in the average Fe–N bond distances of $[\text{Fe}(\text{OEP})(3\text{-Cl-py})_2]\text{ClO}_4$ and molecule 1 of $[\text{Fe}(\text{TPP})(\text{NCS})(\text{py})]$ at the two temperatures is nearly the same. This suggests that the iron(III) center in molecule 1 is involved in an $S = 1/2$, $S = 5/2$ thermal spin equilibrium and is about 50% high-spin at room temperature. Hence, it is reasonable to interpret the structural data in terms of two magnetic sites: a high-spin site (molecule 2) and a spin-equilibrium site (molecule 1).

The variable-temperature magnetic susceptibility data support this hypothesis. The magnetic moment at room temperature is about $5.1 \mu_B$ and decreases to about $4.3 \mu_B$ at 84 K. The decreasing μ_{eff} value corresponds to a change in the spin mixture from about 70% high-spin at 293 K to about 50% at 84 K.²⁰ If the spin state of molecule 2 is taken to be $S = 5/2$ at all temperatures examined, then molecule 1 must be about 50% high spin at room temperature and essentially low spin at 84 K. This two-site interpretation of the data leads to a prediction, namely that unless molecule 2 should start to change its spin state, the

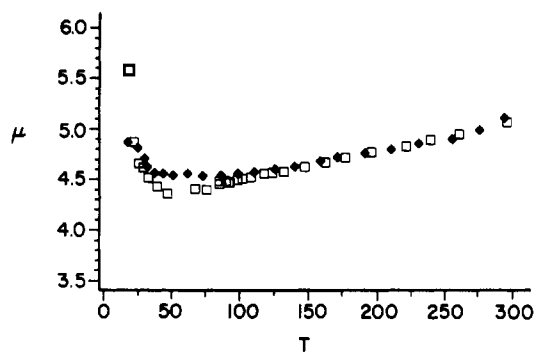


Figure 5. Magnetic moments of the second and third preparations of triclinic $[\text{Fe}(\text{TPP})(\text{NCS})(\text{py})]$ measured between 18 and 293 K.

magnetic moment should remain essentially constant below 84 K. This is in fact observed. As shown in Figure 5, an extension of the magnetic moments of the second sample of $[\text{Fe}(\text{TPP})(\text{NCS})(\text{py})]$ and the magnetic moments of a third sample remain nearly constant from 84 to 25 K. Below 25 K the magnetic moment rises slightly, perhaps as a consequence of a temperature-induced phase change.

The structural results suggest two possible reasons for the site discrimination. As we have noted previously,^{10,21} rotational ligand

(20) The fraction, α , in the high-spin state is calculated by $\mu^2 = \alpha(\mu_{\text{hs}})^2 + (1 - \alpha)(\mu_{\text{ls}})^2$, where $\mu_{\text{hs}} = 5.9$ and μ_{ls} was taken to be $2.4 \mu_B$.

(21) Geiger, D. K.; Lee, Y. J.; Scheidt, W. R. *J. Am. Chem. Soc.* **1984**, *106*, 6339–6343.

orientations can have an effect on the spin state of iron(III) porphyrinates. All known^{9,22} pyridine-complexed low-spin iron(III) porphyrinates have ϕ angles²³ between 40 and 45°. The few remaining derivatives are not low spin and have ϕ values between 0 and 10°. The origin of this orientation effect is in the steric interactions between the pyridine hydrogen atoms and atoms of the core at ϕ values significantly less than 40°: a low-spin axial bond distance (2.03 Å) leads to unreasonably short nonbonded distances. With the foregoing background, we were not surprised to find that the ϕ value for molecule 1, the spin-equilibrium site, is 44°. Molecule 2, the high-spin site, has $\phi \approx 30^\circ$. A second feature that probably weakens the axial ligand field in molecule 2, and hence favors a high-spin state, is the deviation from ideal coordination modes of both axial ligands. The FeNCS group is bent with an apparent Fe-N-C angle of 139°. Further, the plane of the pyridine ring is tilted with a dihedral angle between the pyridine plane and the porphyrinato plane of 73°. We have previously noted⁶ that packing interactions appear responsible for a number of nonlinear MNCS groups that are described in the literature. The geometry of the two axial ligands is normal in molecule 1; the Fe-N-C angle is 175° and the dihedral angle between the pyridine plane and the porphyrinato plane is 90°.

Interestingly, some aspects of the nonideal coordination geometry of molecule 2 are found in the structure of (NCS)metHb.³ The Fe-NCS linkage in (NCS)metHb is bent in both subunits. An angle of approximately 120° is observed and is the apparent result of the steric constraints of the heme pocket. It is curious, albeit surely coincidental, that the two molecules in the asymmetric unit of [Fe(TPP)(NCS)(py)] are different magnetically, as is found in the two crystallographically unique hemes in (NCS)-metHb. Although both hemes have a bent thiocyanate, the crystallographic results suggest that the β -heme is high spin and that the α -heme is an equilibrium mixture of high- and low-spin

states.³ However in [Fe(TPP)(NCS)(py)], molecule 1 with the linear Fe-NCS group is involved in the spin equilibrium. The molecule (2) with the bent Fe-NCS is high spin. Further, [Fe(TPP)(NCS)(py)]^{1/2}py is low spin and has a bent Fe-NCS group.⁶ [Fe(OEP)(NCS)(py)] is a high spin and has a linear Fe-NCS group. This lack of correlation between the spin state of the iron(III) center and the Fe-N-C angle suggests that the angle adopted is a result of packing constraints and not π interactions.²⁴

Both molecules have essentially planar porphyrin cores. The dihedral angles formed by the peripheral phenyl rings and the porphyrinato core are 89 and 72° for molecule 1 and 55 and 80° for molecule 2. All are within the normal range.

Summary

The two crystallographically unique molecules in the asymmetric unit of the triclinic phase of [Fe(TPP)(NCS)(py)] exhibit different magnetic behavior. Although the axial ligands are the same, one molecule is high spin and the other is an equilibrium mixture of high- and low-spin states. The two-site interpretation of the magnetic data is independent of the choice of space group. This [Fe(TPP)(NCS)(py)] system further exemplifies the importance of heme environment in determining spin state in (porphyrinato)iron(III) complexes.

Acknowledgment. We thank the National Institutes of Health for support of this work under Grant HL-15627.

Registry No. [Fe(TPP)(NCS)(py)], 81602-84-8; Fe(TPP)(NCS), 81877-32-9.

Supplementary Material Available: For [Fe(TPP)(NCS)(py)] at 293 K, Figures 1S and 2S, ORTEP plots of the molecular structure, Table A, final anisotropic temperature factors, Table B, fixed hydrogen atom positions, Table C, rigid-group parameters and derived crystallographic coordinates for the axial ligands, and a table of observed and calculated structure amplitudes ($\times 10$) and for [Fe(TPP)(NCS)(py)] at 96 K, Table D, final anisotropic thermal parameters, Table E, fixed hydrogen positions, Table F, rigid-group parameters and derived crystallographic coordinates for the axial ligands, and a table of observed and calculated structure amplitudes ($\times 10$) (56 pages). Ordering information is given on any current masthead page.

(22) Adams, K. M.; Rasmussen, P. G.; Scheidt, W. R.; Hatano, K. *Inorg. Chem.* 1979, 18, 1892-1899. Scheidt, W. R.; Lee, Y. J.; Luangdilok, W.; Haller, K. J.; Anzai, K.; Hatano, K. *Inorg. Chem.* 1983, 22, 1516-1522.

(23) The ϕ value has been defined as 0° when the projection of the planar axial ligand eclipses the M-N₂ bond and 45° when the projection eclipses the metal-methine carbon vector.

(24) Drew, M. G. B.; Othman, A. H.; Nelson, S. M. *J. Chem. Soc., Dalton Trans.* 1976, 1394-1399.

Contribution from the Department of Chemistry, University of California, and Materials and Molecular Research Division, Lawrence Berkeley Laboratory, Berkeley, California 94720

π -Donor Character of the Dimethylamido Ligand

Richard A. Andersen, David B. Beach, and William L. Jolly*

Received July 31, 1985

The core electron binding energies of dimethylamides of early transition metals, when qualitatively interpreted in terms of atomic charges, are consistent with nitrogen-metal $p\pi \rightarrow d\pi$ bonding. Further support for such π bonding is obtained by the "localized orbital ionization potential" method, in which one compares the nitrogen lone-pair ionization potentials with the ionization potentials that the nitrogen 2p orbitals would have if they were strictly nonbonding.

Structural data for transition-metal amides show that the nitrogen atom of a terminal amido ligand generally has a planar or almost planar three-coordinate environment. In addition, the M-N distance is usually shorter than the predicted single-bond distance. These observations are usually interpreted as evidence for significant $p\pi \rightarrow d\pi$ bonding between the nitrogen and transition-metal atoms.¹ However, the data are not unequivocal because the length of an M-N single bond is not known experimentally. In addition, the structural features might be due to ionic bonding, with a tight, head-on orientation of the NR₂⁻ dipole.

In this study we have determined the core electron binding energies of the metal, nitrogen, and carbon atoms in seven homoleptic dimethylamido complexes of the early transition metals. These data can be used to ascertain the importance of N-M $p\pi \rightarrow d\pi$ bonding in two ways. First, the data can be used qualitatively to estimate the relative magnitudes of atomic charges, and these atomic charge data can be interpreted in terms of possible $p\pi \rightarrow d\pi$ bonding. Second, the localized orbital ionization potential (LOIP) method can be used.^{2,3} That is, the core binding energies can be used to estimate what the nitrogen lone-pair ionization potentials would be if the lone pairs were strictly

(1) Lappert, M. F.; Power, P. P.; Sanger, A. R.; Srivastava, R. C. "Metal and Metalloid Amides"; Halsted Press/Wiley: New York, 1980; pp 19-21, 468, 477 ff.

(2) Jolly, W. L. *Acc. Chem. Res.* 1983, 16, 370.

(3) Jolly, W. L. *Chem. Phys. Lett.* 1983, 100, 546.